

## Tuning the chiroptical and morphological properties of steroidal-porphyrin aggregates: a mechanistic, structural, and MM investigation†

Cite this: *Org. Biomol. Chem.*, 2014, **12**, 3956

Chiara Lorecchio,<sup>a</sup> Mariano Venanzi,<sup>a</sup> Claudia Mazzuca,<sup>a</sup> Raffaella Lettieri,<sup>a</sup> Antonio Palleschi,<sup>\*a</sup> Thu Huong Nguyen Thi,<sup>b</sup> Lenka Cardová,<sup>c</sup> Pavel Drasar<sup>c</sup> and Donato Monti<sup>\*a</sup>

The aggregation of a steroid-functionalised porphyrin derivative occurs with the formation of J-type chiral species. Spectroscopic and SEM studies indicate that the initial concentration of the macrocycle strongly influences the morphology of the final mesoscopic structures, as a consequence of a change in the mechanistic course of the self-assembly process. Fibrillar structures are obtained at low porphyrin concentration, whereas aggregates of globular shapes are formed on increasing the substrate concentration. Molecular mechanics investigations gave insights into the intimate nature of the driving forces that govern the self-assembly process, pointing out the importance of ring distortion, of intramolecular steroidal OH– $\pi$  hydrogen bonds, as well as dispersion forces among the tetrapyrrolic platforms.

Received 18th January 2014,  
Accepted 10th April 2014  
DOI: 10.1039/c4ob00134f  
www.rsc.org/obc

### Introduction

Steroidal-porphyrin derivatives are of interest owing to their application in many fields, such as, among others, molecular recognition,<sup>1</sup> catalysis,<sup>2</sup> biomimetic machineries,<sup>3</sup> and medicine.<sup>4</sup> Our interest in this class of molecules<sup>5</sup> sprung from their ability to yield, under particular conditions, extended aggregates featuring supramolecular chirality.<sup>6</sup> The supramolecular chirogenesis is the result of the presence of the steroid groups, which drive the self-assembly process to the formation of chiral suprastructures.<sup>7</sup> The strong aggregation propensity of these compounds is endowed by the extended  $\pi$ -electronic distribution of the porphyrin scaffold.

In the present work we have undertaken a deep study of the aggregation properties of a cholic-acid appended porphyrin derivative (**H<sub>2</sub>CholP**; Chart 1), with the aim to investigate the effect of the reaction conditions on the chiroptical features of the final suprastructures and on the mechanism of their formation. Molecular mechanics (MM) investigation has also been performed in order to gain information on the intimate

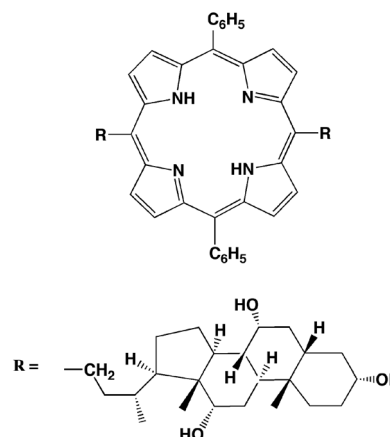


**Chart 1** Molecular structure of the porphyrin **H<sub>2</sub>CholP** studied in the work.

nature of the forces that govern the formation of the supramolecular chiral assemblies. We may anticipate that the cholic moieties, owing to their bowl-conformation with one polar face (three hydroxyl groups) and an extended hydrophobic area, play a fundamental role in the self-assembly process.

## Results and discussion

### Aggregation studies

The title cholic-acid based porphyrin has been prepared and fully characterised by following published procedures. Methyl

<sup>a</sup>Dipartimento di Scienze e Tecnologie Chimiche, Università di Roma Tor Vergata, Via della Ricerca Scientifica 1, 00133 Rome, Italy. E-mail: monti@stc.uniroma2.it; Fax: +39 067259 4328; Tel: +39 067259 4738

<sup>b</sup>Department of Chemistry, Faculty of Science, Purkyně University, Ústí nad Labem, České mládeže 8, 400 96 Ústí nad Labem, Czech Republic

<sup>c</sup>Department of Natural Compounds Chemistry, Institute of Chemical Technology Prague, Technická 5, 166 28 Prague 6, Czech Republic

†Electronic supplementary information (ESI) available: Details of MM calculations and figures cited in the text. See DOI: 10.1039/c4ob00134f



cholate was condensed with pyrrolyl magnesium bromide to give the dipyrrolylsteroid precursor that was subjected to Lindsey condensation with benzaldehyde and oxidation with DDQ.<sup>8</sup> The molecular structure of the final product is shown in Chart 1. The two appended steroidal moieties, owing to the presence of three hydroxyl groups, imbue the whole structure with an amphiphilic character, allowing for some solubility in aqueous solvents. Moreover, these groups should act as *chiral effectors* during the recognition process, which is initiated during the formation of self-assembled supramolecular aggregates.<sup>9</sup>

Aggregation studies have been carried out in water-dimethylacetamide (DMA) solvent mixtures at micromolar concentrations.<sup>‡</sup> In all cases the samples have been prepared by following the same protocol consisting of the addition to a pre-formed solution of the porphyrin in DMA of the amount of water to give the investigated solvent composition. In DMA rich solvents the porphyrin is in monomeric form, with the Soret band featured at 417 nm. The increase of water content fosters the aggregation process, as indicated by a typical red shift of the Soret band to *ca.* 430 nm, along with a strong hypochromic effect and band broadening. The bathochromic shift indicates the formation of aggregates with a J-type morphology.<sup>10</sup> The extent of aggregation depends on the solvent composition, being complete at water proportion higher than 40% (v : v).

### Kinetic studies

Kinetic studies were carried out with a DMA–H<sub>2</sub>O solvent mixture of 58 : 42 (v : v) as this precise solvent composition gave optimal reaction rates, that are conveniently monitored by conventional spectroscopic means, and good solubility of the substrate. A precise protocol for preparation of the solution has been strictly followed, consisting in the addition of the required amount of water to a preformed porphyrin solution in DMA (see the Experimental section). This ensures the highest reproducibility of the spectral and mechanistic results.<sup>11</sup> At higher water proportion the reaction is complete within the time required for the preparation of the samples, whereas in richer organic solvent media, the aggregation rates are too low for an accurate evaluation of the data. The concentrations of the porphyrin span one order of magnitude, from 3.0 to 10  $\mu$ M. All UV-Vis spectra showed a clear isosbestic point at *ca.* 422 nm, indicating that equilibrium between monomers and aggregates of similar morphologies actually takes place (Fig. 1, left), with no evidence of formation of intermediate species.

The aggregation features are strongly dependent on the initial concentration of the macrocycle. The aggregation at low concentration (*i.e.* from 3 to 5  $\mu$ M) showed a peculiar biphasic behaviour, in which an initial aggregation process is followed

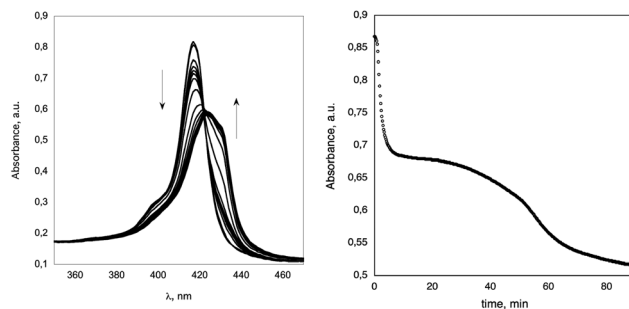


**Fig. 1** (Left) spectral variation of H<sub>2</sub>CholP ( $3.0 \times 10^{-6}$  M) with time in DMA–H<sub>2</sub>O 58 : 42 (v : v) at  $T = 298.15$  K. (Right) corresponding kinetic plot followed at  $\lambda = 417$  nm.

by a slower step, likely involving a structural rearrangement of the first-formed species. This is represented in Fig. 1, right, in which the changes of the Soret band absorption maximum at  $\lambda = 417$  nm are reported against time.

The analysis of the kinetic decay has been carried out according to the following equation, successfully employed in the case of porphyrin aggregation on chiral templates:<sup>12</sup>

$$\text{Abs}_t = \text{Abs}_\infty + \Delta\text{Abs}_1 \exp(-k_1 t)^{\beta_1} + \Delta\text{Abs}_2 \exp(-k_2 t)^{\beta_2} \quad (1)$$

where  $\text{Abs}_t$  is the observed absorbance at a given time,  $\text{Abs}_\infty$  is the absorbance at infinite time (*i.e.* reaction completion), and  $\Delta\text{Abs}_i$ ,  $k_i$  and  $\beta_i$  are the absorbance changes for the two stages, their rate constant values and the associated exponential factors, respectively. A stretching factor  $\beta > 1$  indicates the occurrence of a cooperative process, whereas a value  $\beta < 1$  indicates a diffusion-limited phenomenon. A value of  $\beta = 1$  indicates a reaction-limited (*i.e.* first-order) process. The data are reported in Table 1. In the cases considered, both the steps are characterised by a high degree of cooperativity, with the first step being faster than the second one, by about one order of magnitude. As far as the first step is concerned, the rate constant values increase with increasing the initial porphyrin concentration. Conversely, the rate constant of the second step is almost independent of the porphyrin concentration.

Recent examples of stepwise formation of aggregate species have been reported. Borissevitch showed that in the acid-fostered aggregation of a water-soluble tetra-sulphonatophenyl porphyrin, initially formed structures with face-to-face H morphology evolve into J-type ones with time.<sup>13</sup> The same behaviour has been observed in the case of water insoluble

**Table 1** Kinetic parameters for the aggregation of H<sub>2</sub>CholP<sup>a</sup>

[H <sub>2</sub> CholP] ( $\mu$ M)	$k_1/10^{-3} \text{ s}^{-1}$	$k_2/10^{-4} \text{ s}^{-1}$	$\beta_1$	$\beta_2$
3.0	5.9 ( $\pm 0.1$ )	4.9 ( $\pm 0.1$ )	1.91 ( $\pm 0.09$ )	3.64 ( $\pm 0.05$ )
5.0	8.9 ( $\pm 0.1$ )	4.1 ( $\pm 0.1$ )	1.83 ( $\pm 0.03$ )	3.92 ( $\pm 0.03$ )
10.0 <sup>b</sup>	12 ( $\pm 1$ )		0.56 ( $\pm 0.01$ )	
10.0 <sup>b,c</sup>	13 ( $\pm 1$ )		0.63 ( $\pm 0.04$ )	

<sup>a</sup> In DMA–H<sub>2</sub>O 58/42% (v : v) at  $T = 298.15$  K; followed by UV-Vis spectroscopy ( $\lambda = 417$  nm); values calculated according to eqn (1).

<sup>b</sup> Values calculated according to eqn (2). <sup>c</sup> Followed at  $\lambda = 430$  nm.

<sup>‡</sup> Preliminary aggregation studies have been reported in ref. 8. We choose this particular solvent mixture as it allows for the best reproducible results, solubility, and stability of the porphyrin solute compared to other systems such as acetonitrile–water or DMSO–water.



thiophene-based dendritic porphyrin. In this case the kinetics of H- to J-form conversion depends on the degree of branching, being slower for a higher-generation derivative, owing to its more favourable  $\pi$ - $\pi$  self-interaction.<sup>14</sup>

In our case, according to the UV-Vis spectral changes, we observed only an initial formation of aspecific structures (broadening and hypochromic effect, with no absorbance shift), which subsequently rearrange themselves into specific red-shifted J-type forms. We may surmise that an initial faster interaction occurs, governed by  $\pi$ - $\pi$  and London dispersion forces, followed by a structural slower rearrangement at the molecular level, dictated by subtle factors such as intramolecular hydrogen bonds and plane distortions due to the peculiar structure of the cholic moieties. These structural rearrangements bias then a specific geometry of interaction at the supra-molecular level, leading to the final ordered suprastructures. This hypothesis has been corroborated by further CD and MM studies (*vide infra*).

A change of mechanism is found on further increase of the concentration of the substrate. By carrying out the aggregation at 10  $\mu$ M, for example, only a single evolution step is observed (Fig. 2). In this case the data can be fitted by a stretching exponential equation (eqn (2)). This finding indicates the occurrence of a diffusion limited aggregation process (DLA) that implies the formation of aggregate clusters that grow by further inclusion of monomers. This mechanism has been reported in the literature to be operative in the random growth of systems constituted by clusters of solid particles (*e.g.* metals and latex).<sup>15</sup>

$$\text{Abs}_t = \text{Abs}_0 + (\text{Abs}_\infty - \text{Abs}_0)[1 - \exp(-kt)^\beta] \quad (2)$$

where Abs,  $k$  and  $\beta$  have the usual meaning. However, in this precise case the stretching factor  $\beta$  is required to be  $<1$ .

Evidently the increase of the concentration favours the rapid formation of aggregation nuclei, likely constituted by a small number of macrocycle units, slowly evolving into larger forms. We recently observed a similar behaviour in the aggregation of a related steroid appended porphyrin,<sup>5a,16</sup> in which the increase of concentration biases a change of mechanism from autocatalytic to a diffusion controlled one. The kinetic

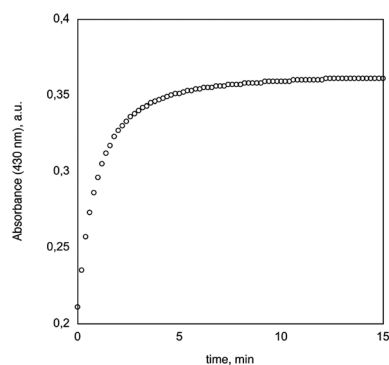


Fig. 2 Kinetic plot ( $\lambda = 417$  nm) of the aggregation of porphyrin  $\text{H}_2\text{CholP}$  ( $1.0 \times 10^{-5}$  M) in DMA- $\text{H}_2\text{O}$  58 : 42 (v : v) at  $T = 298.15$  K.

parameters of the complete aggregation process are reported in Table 1.

It is worth noting that, as reported in the case of the experiment carried out at 10  $\mu$ M concentration, the calculated kinetic parameters obtained by following the spectral evolution at different wavelengths are identical within the experimental errors, ruling out the formation of intermediate species during the aggregation process.

Changes in porphyrin aggregation mechanisms have recently been reported in the literature. This can be the effect of the increase of the macrocycle concentration, or an effect of the change in bulk solvent properties, such as the ionic strength or pH of the solution, as found for acid fostered aggregation of charged water-soluble species.<sup>17</sup> All these factors may have a strong influence on the critical stage of monomer nucleation, biasing the mechanistic course of the process. In our case we may surmise that the increase of the initial monomer number in solution favours the formation of small porphyrin clusters that successively grow by random inclusion of further macrocycles (DLA mechanism).

### Circular dichroism studies

Circular dichroism spectroscopy studies showed that the aggregation occurs with the formation of chiral suprastructures. This is certainly due to the interaction of the steroid chiral moieties that imprint an overall asymmetry to the growing species. In all of the cases considered, the aggregation occurs with formation of chiral suprastructures, as indicated in Fig. 3, left, which shows the time evolution of the CD spectrum, for the aggregation carried out at 3  $\mu$ M concentration. The observed complex spectral pattern results from the superimposition of two coupled bands; the one at lower energy ( $\lambda_{\text{max}} = 426$  nm) is more intense and shows a  $-/+$  sign, while the band at higher energy ( $\lambda_{\text{max}} = 420$  nm) is less intense and features a  $-/+$  spectral profile. This pattern, according to studies recently reported in the literature,<sup>18</sup> indicates the formation of porphyrin architectures with a rod-like morphology, in which the J-aggregate species show excitonic coupling along preferential space directions.<sup>19</sup> Moreover, a careful comparison with the UV-Vis results obtained under the same reaction conditions gave useful insights for the full comprehension of the phenomena involved.

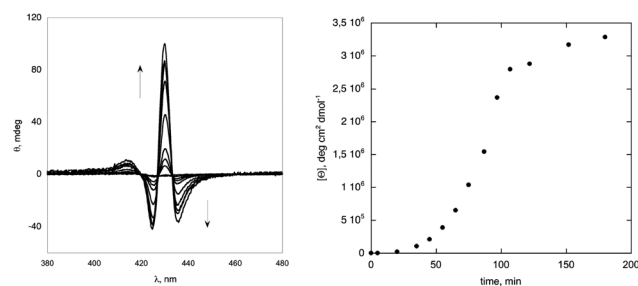


Fig. 3 (Left) CD spectral variation of  $\text{H}_2\text{CholP}$  ( $3.0 \times 10^{-6}$  M) with time in DMA- $\text{H}_2\text{O}$  58 : 42 (v : v) at  $T = 298.15$  K. (Right) corresponding kinetic plot for the reaction followed at  $\lambda = 426$  nm.



A plot of the maximum of CD intensities (*e.g.* at 426 nm) *vs.* time reveals that an appreciable dichroic signal arises from the background only after an initial induction time, which corresponds to the completion of the first aggregation stage observed by UV-Vis spectroscopy (Fig. 3, right). This should imply that in this faster initial step only aspecific non-chiral species are formed. These species subsequently evolve into structures possessing supramolecular chirality during the slower second step, which should then imply a molecular rearrangement of the initially formed structures. Moreover, the intensities of the CD signals, although showing the same pattern, strongly depend on the aggregation conditions. The species formed at lower concentration (*i.e.* a biphasic kinetic regime) in fact feature CD bands showing higher intensities up to four orders of magnitude with respect to those formed at higher concentration, upon DLA mechanism (*i.e.* from *ca.*  $3 \times 10^6$  to  $150 \text{ deg cm}^2 \text{ dmol}^{-1}$ ).

These findings clearly indicate that the spectral pattern, although of reduced intensity, is retained on changing the aggregation mechanism. This indicates constancy of the local geometry of interaction, although of reduced strength, due to an increase of the platform mutual distance that causes a reduction of the coherence length (*i.e.* the number of electronically coupled macrocycles).<sup>20</sup> The formation of structures with looser porphyrin-to-porphyrin interaction should be safely attributed to an effect of steric hindrance that increases in importance on increasing the monomer concentration. In chirally-templated aggregation studies of water-soluble derivatives reported by others<sup>17b</sup> the increase of porphyrin concentration causes a structural change of the aggregates from fractal to rod shape, with a concomitant inversion of the CD spectral pattern. On further increasing the porphyrin concentration, smaller rod-type structures are formed, due to a reduced steric hindrance. The local structural change has been inferred to the effect of the electrostatic repulsion between the charged porphyrins that increases with increasing concentration.<sup>21</sup> In our case of uncharged moieties, this effect should be not operative, leading to constancy of the local symmetry. It is worth noting that the CD spectral pattern observed is different from those of related steroid-porphyrin derivatives studied by our group,<sup>5,16</sup> indicating the crucial effect of the structure and the number of substituents on the periphery of the macrocycles.

### Scanning electron microscopy (SEM) studies

Scanning electron microscopy studies have been carried out in order to acquire information on the morphology of the supramolecular species obtained. The results have been reported in Fig. 4, in which the strong differences in overall morphology of the species obtained at different concentrations are highlighted. The samples have been prepared by simple filtration of the solutions of the aggregates through nylon filters, with a cut-off of  $0.45 \text{ }\mu\text{M}$  (see the Experimental section). In all cases the filtrate solutions did not show any residual porphyrinic material, as indicated by UV-Vis check (Soret band). At lower concentrations (*i.e.* from 3 to  $5 \text{ }\mu\text{M}$ ), where biphasic kinetics is

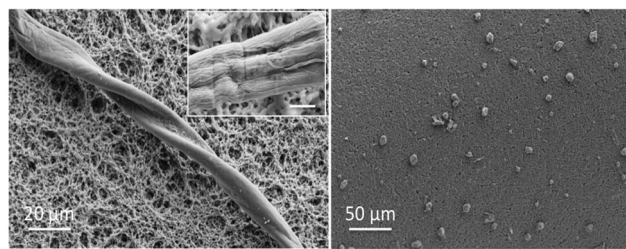


Fig. 4 SEM images of the aggregate obtained in DMA–H<sub>2</sub>O 58:42 (v:v) at H<sub>2</sub>CholP  $3.0 \times 10^{-6} \text{ M}$  (left inset: enlargement of a structure obtained under the same conditions, scale bar  $5 \text{ }\mu\text{m}$ ); at  $1.0 \times 10^{-5} \text{ M}$  (right).

observed, large helicoidal structures, hundreds of micrometres long and *ca.*  $20 \text{ }\mu\text{m}$  wide, are obtained (Fig. 4, left). A closer inspection (inset of Fig. 4, left) reveals that the assemblies are composed of bundles of entangled smaller fibrillar structures about  $10 \text{ }\mu\text{m}$  wide. On the other hand, the structures obtained at higher concentration ( $10 \text{ }\mu\text{M}$ ) showed an aspecific globular morphology, with diameters varying approximately from 5 to  $15 \text{ }\mu\text{m}$  (Fig. 4, right). This is certainly due to their different mechanisms of formation (DLA), and this should also explain the highly reduced ellipticity of the corresponding CD spectra. However, the close similarity of the shapes of the dichroic signals that are featured indicates that, in a short range, a similar mutual geometrical arrangement of the porphyrin units is maintained, although with a reduced degree of long-range order.

### Molecular mechanics (MM) studies

MM calculations have been carried out with the aim of gaining information on the nature of the forces that govern the intimate structure of the supramolecular assemblies. We recently took advantage of this method to get structural information about a porphyrin-based metalloenzyme mimic.<sup>22</sup>

The conformational properties of a single porphyrin unit have been investigated adopting the following procedure: (a) the conformers arising from internal rotation around the torsional angles of the side chains linking the steroid to the porphyrin (ESI Fig. 1†) were built up by making use of the rotational isomeric state model according to standard bond angles and lengths; (b) the conformational energy was then optimized minimising the potential energy comprising electrostatic, stretching, bending, non-bonding, hydrogen bond, and torsional interactions, implemented in the MM4 force field.<sup>23</sup> The “apparent relative dielectric constant” of the solvent mixture has been implicitly taken into account in the calculation.† The results showed that the single porphyrin units feature the deepest energy minimum with a distorted structure, caused by the steric hindrance of the bulky steroid groups. Additionally, this distortion allows for the buildup of

† The apparent  $\epsilon_r$  of the DMA–water 58/42 v:v mixture is 70.5; the value is calculated by taking into consideration the dielectric constant values of the pure solvents, weighted by their molar fractions.





two non-conventional H-bonds among the hydroxyl groups of the steroid moieties and the aromatic electronic distribution of two adjacent *meso* phenyl rings and one pyrrole unit of the porphyrin macrocycle (Fig. 5), with a mean distance of 2.93 Å (*O*-phenyl centre of mass) and an angle of 168 deg.

This kind of interaction has been widely recognised to play an effective role in stabilising local 3D structures of proteins,<sup>24a,b</sup> or to act as a “reserve acceptor” in biomolecules.<sup>24c</sup> This interaction and the steric crowding of the steroidal groups cause a deviation of the porphyrin ring of *ca.* 0.12 Å from planarity, reaching a typical saddled conformation.<sup>25</sup> The distortion of the molecular frame from the planarity is usually steered by the out-of-plane coordination of “large metal ions”, as well as nitrogen core protonation, interaction with metal surfaces<sup>26</sup> or, as in our case of a free-base derivative, by the presence of crowded peripheral moieties. Senge and co-workers, for example, reported on the saddling effect of  $\beta$ -alkyl substitution on tetraphenyl porphyrin derivatives, with a deviation of planarity from 0.10 to 0.46 Å, depending on the degree and on the regiochemistry of substitution.<sup>27</sup> It is interesting to note that all these described structural arrangements lead to a molecular structure that is characterized by an extended hydrophobic surface (ESI Fig. 2†), which is prone to interact with other aromatic platforms by  $\pi$ - $\pi$  and London dispersion forces. This strongly corroborates the experimental findings that indicate that the formation of the aggregates is driven by hydrophobic effects, with the solvent playing a pivotal entropic factor.

We repeated the modelling by explicitly considering the interactions with the solvent molecules. The values obtained by considering the limit cases of pure DMA or pure water are very similar to the values obtained by considering the implicit solvent. In the case of pure water, for example, the *O*-phenyl centroid distance is only slightly increased to 3.10 Å by the effect of hydrogen bonding with vicinal water molecules (see ESI Table 1 and Fig. 3† for details). These small variations confirm that the contribution of the solvation is mainly entropic in nature.

As far as the construction of the supra-assemblies is concerned, we initially studied the possible stepwise arrangements

of the platforms taking into account their well-recognised tendency to aggregate by means of  $\pi$ - $\pi$  interactions. In particular, we started from a parallel disposition of the two macrocycles by varying the initial position of the centres of mass and the relative orientation. For each starting point, during the process of energy minimization, the two porphyrins can translate or rotate without constraints. Due to the steric hindrance of the two steroid groups, the porphyrin rings can approach each other in a parallel fashion to a bonding distance (*e.g.* less than 10 Å) only if they are mutually rotated by about 90 degrees. For example, the minimum energy structure of the dimer shows a distance between the macrocycle platforms of 5.06 Å in good agreement with the typical values that are often found in X-ray structures of solid-state assemblies of related species.<sup>28</sup> Remarkably, this interaction fosters the final structure to reach a J-type arrangement, as also indicated by the red-shifted bands of the UV-Vis spectra of the aggregates, and impresses a supramolecular helicity to the growing architecture. The intramolecular H-bond is maintained ( $d = 3.28$  Å; 155 deg), while the ring distortion is further increased to a value of 0.36 Å.

We used this energy-minimised dimeric motif to build up a multimeric structure. As expected, after the subsequent energy minimization, the structure preserves the local main features, that is: (i) similar distances among the porphyrin planes; (ii) the J-type arrangement; (iii) intramolecular HBs, and (iv) similar ring distortion from the planarity. During the assembly process, the energy per monomer value improves, increasing the number of building blocks, and it tends to a plateau when the contribution of the first and last porphyrins becomes negligible, namely at 20 macrocycle units (ESI Fig. 4†), corresponding to a final stabilisation energy of about 155 kJ mol<sup>-1</sup>. Multimers are arranged to form, on average, a right-handed helix that has a monomeric repeat of  $5.08 \pm 0.50$  Å, and a number of monomers per turn equal to  $5.5 \pm 0.5$  (Fig. 6). The values are in good agreement with those reported for related porphyrin chiral suprastructures possessing two amino acid derivatives in the *meso*-position of the periphery of the ring.<sup>29</sup>

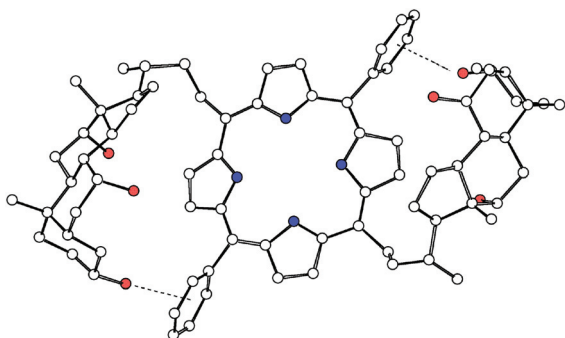


Fig. 5 Minimum energy structure of the porphyrin monomer, evidencing the non-conventional H-bonds between the steroid moieties and the *meso*-phenyl groups (hydrogen atoms are omitted for clarity).

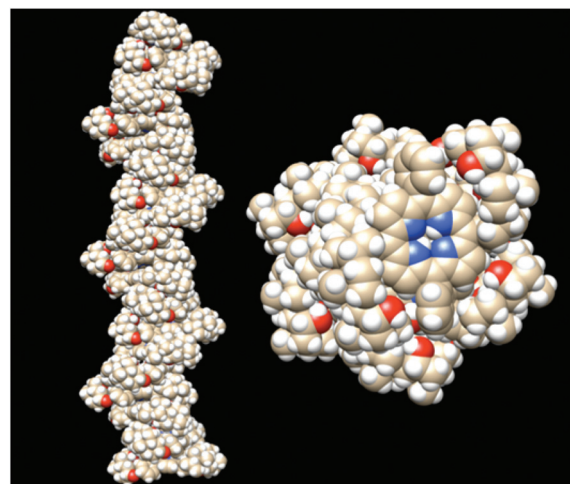


Fig. 6 Lateral (left) and top (right) view of the 20-mer structure.



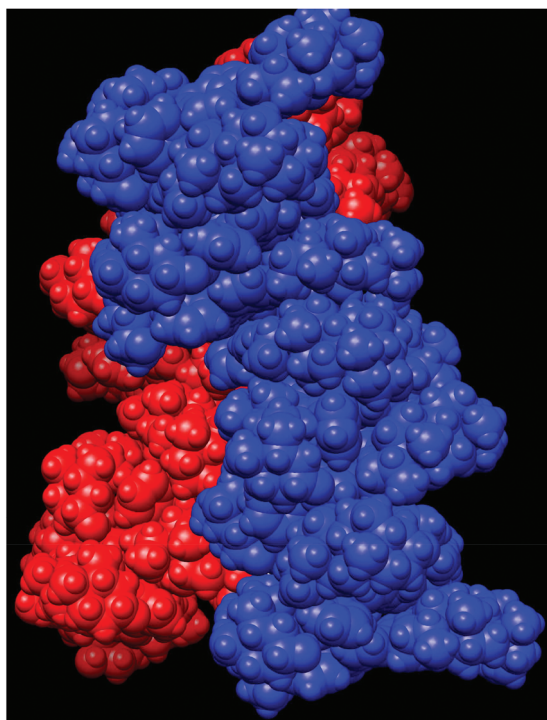


Fig. 7 Calculated structure of two supercoiled decamers after energy minimisation.

In the latter case the energy per molecule is about  $242 \text{ kJ mol}^{-1}$ . The higher value reported can be accounted for by the closer approach of the porphyrin planes ( $4.6 \text{ \AA}$ ), due to the reduced steric crowding of the aminoacid residues with respect to that of the steroid moieties present in **H<sub>2</sub>CholP**.

Finally, we studied the interaction of two right-handed helical decamers, as a basic model for the fibrillar assemblies observed by SEM images, starting from their symmetric helices. We observed a spontaneous tendency of the structures to wrap to form a superhelix, optimising the non-bonding interactions between the external hydrophobic surfaces, with a further energy gain of about  $53 \text{ kJ mol}^{-1}$  (Fig. 7). This additional gain of energy should constitute the driving force for the assembly of the mesoscopic structures observed by SEM microscopy.

## Experimental

### General

Spectroscopic measurements were performed on a Varian Cary 1E spectrophotometer at room temperature unless otherwise indicated. CD spectra were recorded on a JASCO J-600 spectrometer with the cell holder thermostated at  $298 \text{ K}$  and purged with ultrapure nitrogen. All the solvents employed are of spectroscopic grade and used as received. Distilled water used for kinetic and spectroscopic purposes was of Milli-Q (Millipore) grade. The porphyrin stock solutions were prepared by dissolving an appropriate amount of porphyrin in the required

volume of DMA to give the final concentration on the order of  $10^{-3}$  to  $10^{-4} \text{ M}$ . The solutions obtained, used within one week of preparation, were passed through nylon syringe filters (Albet®;  $0.45 \text{ }\mu\text{m}$  porosity) prior to use.

### Synthesis

The porphyrin derivative (5,15-bis(3a,7a,12a-trishydroxy-24-nor-5 $\beta$ -cholan-23-yl)-10,20-diphenylporphyrin) used in the work has been synthesized by following published procedures.<sup>8</sup>  $\text{Log } \epsilon$  (DMA;  $\lambda_{\text{max}}$   $417 \text{ nm}$ ):  $1.21 \times 10^5 \text{ l mol}^{-1} \text{ cm}^{-1}$ .

### Aggregation and kinetic studies

Suitable solutions for aggregation (UV-Vis and CD) and kinetic studies were prepared as follows. Aliquots of porphyrin stock solution (e.g. 15 to  $50 \text{ }\mu\text{L}$  of  $1 \text{ mM}$  stock solution) were added to an appropriate amount of DMA in a  $4 \text{ mL}$  glass vial to obtain solutions with the needed concentration of  $\mu\text{M}$  range. To this solution an exact amount of water was added to obtain the required solvent composition, and the resulting solution was vigorously shaken to ensure homogeneity of the sample. A ca.  $3 \text{ mL}$  portion was transferred into a  $1 \text{ cm}$  quartz cuvette and the relative spectra acquired. In the case of faster reactions the solutions for the kinetic experiment were directly prepared in the cuvette. The kinetic parameters were obtained by a non-linear least-square regression fit (Kaleidagraph® program, Synergy Software, 2003) over hundreds of experimental data points. Entry absorbance values used for the calculations were obtained under non-aggregative conditions (e.g.  $80:20 \text{ DMA-water}$ , v:v) and on completion of the aggregation process. The calculated values showed good correspondence to the experimental ones, indicating the validity of the equations used for the fitting procedure. The kinetic experiments were run in duplicate and the results obtained were in good agreement within the experimental error ( $\pm 5\%$ ;  $r^2 \geq 0.9992$ ). The  $k_i$  and  $\beta_i$  entry values relative to the biphasic kinetics were obtained by performing separated non-linear regression for the two aggregation steps. Once obtained, these values were used as entries for the whole combined eqn (1). The parameters have been further adjusted one at a time, until the best  $r^2$  value was achieved. A final run was then performed to give the results, as reported in Table 1 ( $r^2 \geq 0.9991$ ).

### SEM studies

The samples have been prepared by simple filtration of the solutions of the aggregates through nylon filters with a cut-off of  $0.45 \text{ }\mu\text{m}$ . The filter surfaces have been subsequently analysed by means of an FE-SEM LEO/Supra 35 instrument.

## Conclusions

In conclusion we may summarise that the steroid-functionalised porphyrin derivative studied in this work undergoes a transformation into chiral J-type aggregates in mixed DMA-water solvent mixtures. The morphology of the species obtained strongly depends on the aggregation mechanism,



which is in turn modulated by the initial concentration of the porphyrin building blocks. MM calculations point out the striking role of the hydrophobic effect, as well as the onset of hydroxyl-aromatic interactions, in the overall driving forces that govern the chiral self-assembly process. The results obtained will be of importance also for the study of the origin of the homochirality and chiral amplification in synthetic and natural systems.<sup>30</sup>

## Acknowledgements

The funding of this research by the Italian Ministry for Education, University and Research (PRIN209Z9ASCA and PRIN2010 2010FM738P) and by the Czech Ministry of Education (MSM 6046137305) is gratefully acknowledged.

## Notes and references

- 1 S. Thomas and L. Milanesi, *J. Am. Chem. Soc.*, 2009, **131**, 6618; M. Dukh, D. Šaman, K. Lang, V. Pouzar, I. Černý, P. Drašar and V. Král, *Org. Biomol. Chem.*, 2003, **1**, 3458.
- 2 J. T. Groves and R. Neumann, *J. Am. Chem. Soc.*, 1989, **111**, 2900; J. Lahiri, G. D. Fate, S. B. Ungashe and J. T. Groves, *J. Am. Chem. Soc.*, 1996, **118**, 2347.
- 3 T. S. Balaban, N. Berova, C. M. Drain, R. Hauschild, X. Whang, H. Kalt, S. Lebedkin, J.-M. Lehn, F. Nifaitis, G. Pescitelli, V. I. Prokhorenko, G. Riedel, G. Smeureanu and J. Zeller, *Chem. – Eur. J.*, 2007, **13**, 8411; R. Fong, D. I. Schuster and S. R. Wilson, *Org. Lett.*, 1999, **1**, 729.
- 4 E. Girgenti, R. Ricoux and J.-P. Mahy, *Tetrahedron*, 2004, **60**, 10049.
- 5 (a) K. Zelenka, T. Trnka, I. Tišlerová, D. Monti, S. Cinti, M. L. Naitana, L. Schiaffino, M. Venanzi, G. Laguzzi, L. Luvidi, G. Mancini, Z. Nováková, O. Šimák, Z. Wimmer and P. Drašar, *Chem. – Eur. J.*, 2011, **17**, 13743; (b) R. Lettieri, D. Monti, K. Zelenka, T. Trnka, P. Drašar and M. Venanzi, *New J. Chem.*, 2012, **36**, 1246; (c) H. A. Zhylitskaya, V. N. Zhabinskii, R. P. Litvinovskaya, R. Lettieri, D. Monti, M. Venanzi, V. A. Khripach and P. Drašar, *Steroids*, 2012, **77**, 1169.
- 6 V. V. Borovkov and Y. Inoue, *Top. Curr. Chem.*, 2006, **265**, 89.
- 7 D. Monti, *Top. Heterocycl. Chem.*, 2014, **33**, 231.
- 8 T. H. Nguyen Thi, L. Cardová, M. Dvořáková, D. Ročková and P. Drašar, *Steroids*, 2012, **77**, 858.
- 9 D. Monti, M. De Rossi, A. Sorrenti, G. Laguzzi, E. Gatto, M. Stefanelli, M. Venanzi, L. Luvidi, G. Mancini and R. Paolesse, *Chem. – Eur. J.*, 2010, **16**, 860; D. Monti, M. Venanzi, M. Stefanelli, A. Sorrenti, G. Mancini, C. Di Natale and R. Paolesse, *J. Am. Chem. Soc.*, 2007, **129**, 6688; D. Monti, M. Venanzi, G. Mancini, C. Di Natale and R. Paolesse, *J. Chem. Soc., Chem. Commun.*, 2005, 2471; D. Monti, V. Cantonetti, M. Venanzi, F. Ceccacci, C. Bombelli and G. Mancini, *J. Chem. Soc., Chem. Commun.*, 2004, 972; P. Štěpánek, M. Dukh, D. Šaman, J. Moravcová, L. Kniežo, D. Monti, M. Venanzi, G. Mancini and P. Drašar, *Org. Biomol. Chem.*, 2007, **5**, 960; D. Monti, E. Gatto, M. Venanzi, G. Mancini, A. Sorrenti, P. Štěpánek and P. Drašar, *New J. Chem.*, 2008, **32**, 2127–2133. Studies on the aggregation of related chiral porphyrin derivatives have been recently reported by other authors. See for example: P. Iavicoli, M. Simón-Sorbed and D. B. Amabilino, *New J. Chem.*, 2009, **33**, 358; B. Nieto-Ortega, F. J. Ramirez, D. A. Amabilino, M. Linares, D. Beljonne, J. T. López Navarrete and J. Casado, *Chem. Commun.*, 2012, **48**, 9147; R. van Hameren, A. M. van Buul, M. A. Castriciano, V. Villari, N. Micali, P. Schön, S. Speller, L. Monsù Scolaro, A. E. Rowan, J. A. A. W. Elemans and R. J. M. Nolte, *Nano Lett.*, 2008, **8**, 253; F. Helmich, C. C. Lee, M. M. L. Nieuwenhuizen, G. C. Gielen, P. C. M. Christianen, A. Larsen, G. Fytas, P. E. L. G. Leclère, A. P. J. H. Schenning and E. W. Meijer, *Angew. Chem., Int. Ed.*, 2010, **49**, 3939; F. Helmich, M. M. J. Smulders, C. C. Lee, A. P. J. H. Schenning and E. W. Meijer, *J. Am. Chem. Soc.*, 2011, **133**, 12238.
- 10 F. Würthner, T. E. Kaiser and C. R. Saha-Möller, *Angew. Chem., Int. Ed.*, 2011, **50**, 3376.
- 11 It has been reported that the protocol of mixing of the reactants is a crucial issue when dealing with kinetic studies of porphyrin aggregation. See for example: P. J. Collings, E. J. Gibbs, T. E. Starr, O. Vafek, C. Yee, L. A. Pomerance, R. F. Pasternack and J. C. de Paula, *Biophys. J. Phys. Chem. B.*, 1999, **103**, 8474; R. F. Pasternack, E. J. Gibbs, P. J. Collings, J. C. de Paula, L. C. Turzo and A. Terracina, *J. Am. Chem. Soc.*, 1998, **120**, 5873; R. F. Pasternack, C. Fleming, S. Herring, P. J. Collings, J. C. de Paula, G. DeCastro and E. J. Gibbs, *Biophys. J.*, 2000, **79**, 50.
- 12 R. Lauceri, G. F. Fasciglione, A. D'Urso, S. Marini, R. Purrello and A. Coletta, *J. Am. Chem. Soc.*, 2008, **130**, 10476.
- 13 L. P. F. Aggarval and I. E. Borisevitch, *Spectrochim. Acta, Part A*, 2006, **63**, 227.
- 14 S. Deng and R. Advincula, *Macromol. Rapid Commun.*, 2011, **32**, 1634.
- 15 T. A. Witten Jr. and L. M. Sander, *Phys. Rev. Lett.*, 1981, **47**, 1400; R. F. Pasternack, C. Fleming, S. Herring, P. J. Collings, J. DePaula, G. DeCastro and E. J. Gibbs, *Biophys. J.*, 2000, **79**, 550; N. Micali, F. Mallamace, A. Romeo, R. Purrello and L. Monsù Scolaro, *J. Phys. Chem. B*, 2000, **104**, 5897.
- 16 M. Naitana, M. Dukh, K. Zelenka, T. Trnka, M. Venanzi, R. Lettieri, P. Drašar and D. Monti, *J. Porphyrins Phthalocyanines*, 2013, **17**, 889.
- 17 (a) L. Monsù Scolaro, M. A. Castriciano, A. Romeo, A. Mazzaglia, F. Mallamace and N. Micali, *Physica A*, 2002, **304**, 158; (b) N. Micali, V. Villari, M. A. Castriciano, A. Romeo and L. Monsù Scolaro, *J. Phys. Chem. B*, 2006, **110**, 8289; (c) F. Mallamace, L. Monsù Scolaro, A. Romeo and N. Micali, *Phys. Rev. Lett.*, 1999, **82**, 3480.
- 18 A. Sorrenti, Z. El-Hachemi, O. Orteaga, A. Canillas, J. Crusats and J. M. Ribó, *Chem. – Eur. J.*, 2012, **18**,





- 8820; M. A. Castriciano, A. Romeo, G. De Luca, V. Villari, L. Monsù Scolaro and N. Micali, *J. Am. Chem. Soc.*, 2011, **133**, 765; M. A. Castriciano, A. Romeo, R. Zagami, N. Micali and L. Monsù Scolaro, *Chem. Commun.*, 2012, **48**, 4872.
- 19 O. Ohno, Y. Kaizu and H. Kobayashi, *J. Chem. Phys.*, 1993, **99**, 4128. It has been also reported by SAXS studies that the presence of both H and J spectral features of water-soluble porphyrin aggregates are due to the formation of hollow cylindrical structures: S. C. M. Gandini, E. L. Gelamo, R. Itri and M. Tabak, *Biophys. J.*, 2003, **85**, 1259.
- 20 The possibility of scaling the chirality in porphyrin aggregates has been recently shown: M. A. Castriciano, A. Romeo, G. De Luca, V. Villari, L. Monsù Scolaro and N. Micali, *J. Am. Chem. Soc.*, 2011, **133**, 756; M. A. Castriciano, A. Romeo, V. Villari, N. Micali and L. Monsù Scolaro, *J. Phys. Chem. B*, 2004, **108**, 9054.
- 21 The same electrostatic effects are implied in the pH-dependent structural rearrangement: M. A. Castriciano, A. Romeo, V. Villari, N. Micali and L. Monsù Scolaro, *J. Phys. Chem. B*, 2003, **107**, 8765.
- 22 M. Venanzi, S. Cianfanelli and A. Palleschi, *J. Pept. Sci.*, 2014, **20**, 36. For related previous studies see also: E. Chiessi, M. Branca, A. Palleschi and B. Pispisa, *Inorg. Chem.*, 1995, **34**, 2600; B. Pispisa, A. Palleschi, M. Venanzi and G. Zanotti, *J. Phys. Chem.*, 1995, **100**, 6835; P. De Santis, S. Morosetti and A. Palleschi, *Biopolymers*, 1983, **22**, 37.
- 23 N. L. Allinger, K. Chen and J.-H. Lii, *J. Comput. Chem.*, 1996, **17**, 642; N. Nevins, K. Chen and N. L. Allinger, *J. Comput. Chem.*, 1996, **17**, 669; N. Nevins, J.-H. Lii and N. L. Allinger, *J. Comput. Chem.*, 1996, **17**, 695;
- N. Nevins and N. L. Allinger, *J. Comput. Chem.*, 1996, **17**, 730.
- 24 (a) T. Steiner and G. Koellner, *J. Mol. Biol.*, 2001, **305**, 535; (b) A. Nallini, K. Saraboji and M. N. Ponnuswamy, *Indian J. Biochem. Biophys.*, 2004, **41**, 184; (c) T. Steiner and G. Koellner, *J. Mol. Biol.*, 2001, **305**, 535.
- 25 For recent overviews on saddled and other non-planar porphyrins see: (a) O. M. Senge, in *The Porphyrin Handbook*, ed. K. M. Kadish, K. M. Smith and R. Guilard, Academic Press, New York, 2000, vol. 1, ch. 6, p. 239; (b) W. R. Scheidt, in *The Porphyrin Handbook*, ed. K. M. Kadish, K. M. Smith and R. Guilard, Academic Press, New York, 2000, vol. 3, ch. 16, p. 49.
- 26 J. Brede, M. Linares, S. Kuck, J. Schwöbel, A. Scarfato, S.-H. Chang, G. Hoffmann, R. Wiesendanger, R. Lensen, P. H. J. Kouwer, J. Hoogboom, A. Rowan, M. Bröring, M. Funk, S. Stafström, F. Zerbetto and R. Lazzaroni, *Nanotechnology*, 2009, **20**, 275602.
- 27 W. W. Kalisch and M. O. Senge, *Tetrahedron Lett.*, 1996, **37**, 1183.
- 28 P. Bhyrappa, S. R. Wilson and K. S. Suslick, *J. Am. Chem. Soc.*, 1997, **119**, 8492. For recent EDXD studies on L-phenyl alanine imprinted chiral porphyrin aggregates see: R. Matassa, M. Carbone, R. Lauceri, R. Purrello and R. Caminiti, *Adv. Mater.*, 2007, **19**, 3961.
- 29 P. Iavicoli, H. Xu, L. N. Feldborg, M. Linares, M. Paradinas, S. Stafström, C. Ocal, B. Nieto-Ortega, J. Casado, J. T. López Navarrete, R. Lazzaroni, S. De Feyter and D. B. Amabilino, *J. Am. Chem. Soc.*, 2010, **132**, 9350.
- 30 A. Guijarro and M. Yus, *The Origin of Chirality in Molecules of Life. A revision from awareness to the current theories and perspectives of this unsolved problem*, RSC Publishing, Cambridge, UK, 2009.

